Temperature dependent EUV spectra of Gd, Tb and Dy ions observed in the Large Helical Device

C Suzuki[1], F Koike[2], I Murakami[1], N Tamura[1], S Sudo[1]

[1] National Institute for Fusion Science, 322-6 Oroshi-cho, Toki 509-5292, Japan
[2] Sophia University, 7-1 Kioi-cho, Chiyoda-ku, Tokyo 102-8554, Japan

E-mail: csuzuki@nifs.ac.jp

Abstract. We have observed a number of different types of extreme ultraviolet (EUV) spectra from highly charged gadolinium (Gd), terbium (Tb) and dysprosium (Dy) ions in optically thin plasmas produced in the Large Helical Device at the National Institute for Fusion Science. Temporal changes in EUV spectra in the 6–9 nm region subsequent to the injections of solid pellets were measured by a grazing incidence spectrometer. The spectra rapidly change from discrete features into unresolved transition arrays (UTAs) following a drop in the electron temperature after the heating power is reduced. In particular, extremely narrowed UTA features, which comprise spectral lines of Ag-like, Pd-like and neighboring ion stages, are observed when the peak electron temperature is less than 0.45 keV due to the formation of hollow plasmas. Some discrete spectral lines of Cu-like and Ag-like ions have been identified in the high and low temperature plasmas, respectively, some of which are experimentally identified for the first time.

PACS numbers: 32.30.Jc, 32.70.-n, 52.25.Os

Submitted to: *J. Phys. B: At. Mol. Opt. Phys.*

1. Introduction

The needs for experimental databases of extreme ultraviolet (EUV) spectra from highly charged heavy ions are recently growing in a variety of fields. In the field of semiconductor industries, for example, EUV lithography at 13.5 nm using laser-produced tin plasmas is now under development, and lanthanide ions are potentially considered as a light source at a shorter wavelength around 6–7 nm [1, 2, 3, 4]. Gadolinium (Gd) and terbium (Tb) have been primarily investigated as promising candidates for bright emitters at wavelengths in the vicinity of 6.7 nm because of the existing multilayer mirrors with high reflectivity in this wavelength region.

The bright EUV emissions mentioned above originate from a quasicontinuum spectral feature composed of numerous lines due to n=4–4 transitions of ions with outermost 4d and 4f subshells. Such a quasicontinuum feature is often referred to as unresolved transition array (UTA), of which the center wavelength moves monotonically to shorter wavelengths as Z increases [5]. Because the UTA features are strongly influenced by multi-electron correlation effects such as configuration interaction [6], studies on EUV spectra from highly charged heavy ions are of great interest also in terms of basic atomic physics. However, modeling of EUV spectra in laser-produced plasmas is generally challenging due to the effects of line broadening and self-absorption. On the other hand, magnetically confined torus plasmas for fusion research containing highly charged heavy ions can provide optically thin, bright light sources and provide a good platform for benchmarking of models because of their low opacity as well as the availabilities of pellet injection systems and reliable electron temperature diagnostics.

In this respect, we have recently performed systematic studies on EUV spectra from highly charged heavy ions in the Large Helical Device (LHD) plasmas at the National Institute for Fusion Science [7, 8, 9, 10, 11, 12, 13]. As to lanthanides, we have already reported some results on Gd and neodymium (Nd) in a recent article [12] in which several distinct types of spectral features are clearly observed depending on the electron temperature. In this article, we present a continuing series of work extended to Tb and dysprosium (Dy), which are also possible candidates for the light source around 6–7 nm, to investigate Z dependence of the spectra as well as Gd.

Though a number of experimental works on EUV spectra from lanthanide ions have been performed so far in laser produced plasmas [1, 14, 15] and vacuum spark discharges [1, 16], higher opacities and less defined spatial distributions of plasma parameters make it difficult to analyze the measured spectra precisely in these plasmas. Some studies on tokamak plasmas have been reported earlier [17, 18, 19, 20]. However, they observed broad UTA spectra blended with some discrete lines because the heavy elements were introduced by laser-blow off technique. Also, discussions on the electron temperature dependence were difficult for lack of precise measurements of electron temperature profiles. In addition, charge-separated spectra of Gd and Dy ions have recently been observed using electron beam ion traps [21, 22, 23]. Nevertheless, basic spectroscopic databases are still incomplete for these highly charged lanthanide ions.

In this work, we have systematically recorded EUV spectra from highly charged Gd, Tb and Dy ions by injecting pellets into LHD plasmas. We specifically focus on drastic change in spectral features depending on the electron temperature, which are similar to the results reported previously for Gd [12]. We have also succeeded to form hollow plasmas in which spectral narrowing of the UTA is clearly observed. Several discrete lines of Cu-like and Ag-like ions were identified in the high and low temperature plasmas, by comparisons with the previous experiments and theoretical calculations. In particular, the lines of Cu-like Tb ions are experimentally identified for the first time in this study. Further analyses of the temperature dependent spectra based on comparisons with collisional-radiative modeling will be reported elsewhere in the future.

2. Experimental

Since the experimental setup used in the present study are basically the same as that described in our earlier article [12], only a brief explanation is given here. The LHD is a large scale device for magnetically confined fusion research equipped with several superconducting coil systems [24]. Small amounts of pure lanthanide powders (Gd, Tb and Dy) are injected by a tracer encapsulated solid pellet (TESPEL) [25, 26] into low density (of the order of 10^{19} m^{-3}) hydrogen plasmas heated mainly by neutral beam injection (NBI) systems. The arrangements of the NBI, the TESPEL injection system and the spectrometer have already been described in [12]. The total amount of the injected lanthanide elements is of the order of 10^{17} atoms. Spatial profiles of electron temperature and density are precisely measured by a laser Thomson scattering diagnostic system [27, 28] which has spatial resolution of about 20 mm and temporal resolution of less than 0.05 s.

EUV spectra are measured by a 2 m Schwob Fraenkel grazing incidence spectrometer [29] equipped with a 600 mm^{-1} grating. The wavelength region is selectable in the range of 1–34 nm by moving the detector along the Rowland circle. The 6–9 nm region where the UTAs of n=4–4 transitions are located was chosen as the observed wavelength band in this study. The line-of-sight of the spectrometer was positioned equatorially in a horizontally elongated cross section of the LHD plasma, similar to the arrangement of the data points of the Thomson scattering diagnostic [9]. Therefore, the measured spectra are line-of-sight integrated along the plasma layers with different electron temperatures. This temperature distribution is determined based on the Thomson scattering data. Temporal evolution of the spectra was recorded with an interval of 0.1 or 0.2 s with an overall spectral resolution of about 0.01 nm. The wavelength calibration was carried out by observing well-known lines of carbon, nitrogen and neon ions in other discharges. As a result, a wavelength uncertainty less than $\pm$0.005 nm can be achieved.

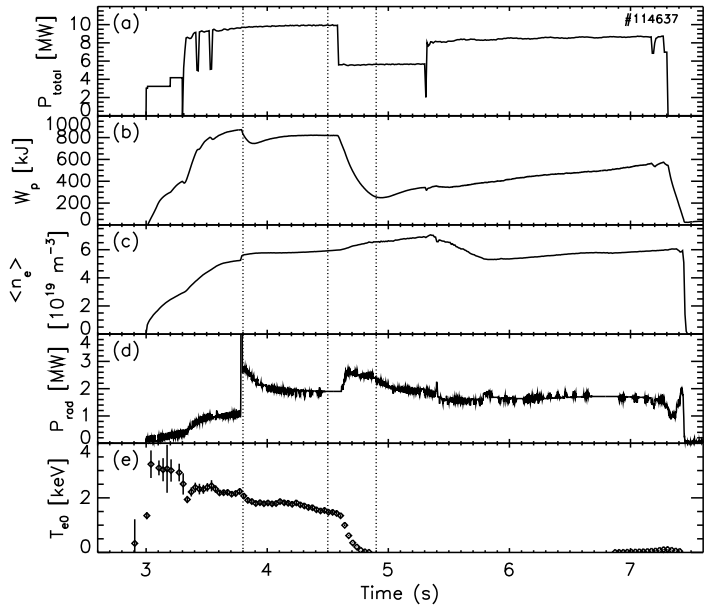

Figure 1. Temporal evolutions of (a) total heating power ($P_{\rm total}$), (b) plasma stored energy ($W_{\rm p}$), (c) line averaged electron density along a line of sight of an interferometer ($\langle n_{\rm e} \rangle$), (d) total radiated power ($P_{\rm rad}$) and (e) central electron temperature ($T_{\rm e0}$) in an LHD discharge with a Tb pellet injected at 3.8 s. The EUV spectra and electron temperature profiles measured during 4.5–4.9 s are shown in figure 2 with a time interval of 0.1 s.

3. Temperature dependent EUV spectra

In the LHD experiments, we can generate plasmas with a wide range of electron temperatures by controlling the heating power and the tracer amount as long as the plasma is not collapsed. In particular, hollow temperature profiles can be obtained by decreasing the heating power after the TESPEL injection as mentioned in our earlier article for Gd and Nd [12]. We have successfully carried out the same procedure for Tb and Dy in this study. Figure 1 shows an example of such a discharge with a Tb pellet injection, where temporal evolutions of total heating power ($P_{\rm total}$), plasma stored energy ($W_{\rm p}$), line averaged electron density along a line of sight of an interferometer ($\langle n_{\rm e} \rangle$), total radiated power ($P_{\rm rad}$) and central electron temperature ($T_{\rm e0}$) are plotted. The discharge was started up by electron cyclotron heating in the early phase (3.0–3.3 s) followed by the NBI heating (3.3–7.3 s). A Tb pellet was injected at 3.8 s where $P_{\rm rad}$ sharply increased. The increase in electron density at the timing of the pellet injection is rather small, which indicates the amount of the injected Tb is quite small. The heating power was reduced to almost one-half at 4.6 s, then the stored energy rapidly dropped until 4.9 s with the extra increase in $P_{\rm rad}$. During this phase, $T_{\rm e0}$ rapidly dropped and the EUV spectrum changed drastically, as is mentioned below.

The temporal evolution of EUV spectrum was measured with 0.1 s intervals

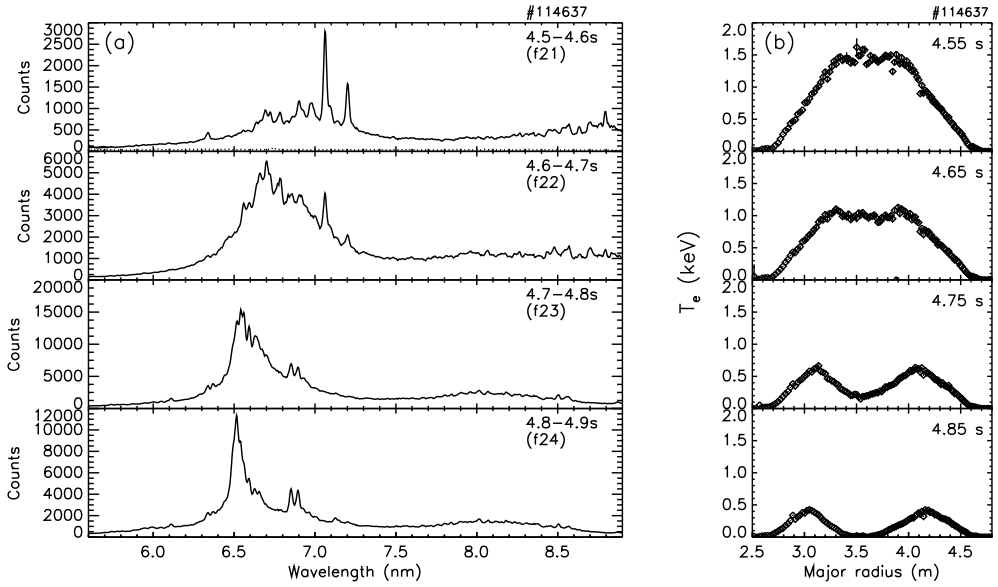

Figure 2. Temporal evolutions of (a) EUV spectrum and (b) electron temperature profile during 4.5–4.9 s in the discharge shown in figure 1. The background spectrum taken just before the pellet injection (3.7–3.8 s) is drawn with a broken line in the top panel of (a), which is negligibly weak.

throughout the discharge. Figure 2 shows temporal evolutions of (a) EUV spectrum and (b) electron temperature profile during 4.5–4.9 s in the discharge shown in figure 1. The intensity of a background spectrum taken just before the pellet injection (3.7–3.8 s) is negligibly low as shown with a broken line in the top panel of figure 2 (a). The peak electron temperature was about 1.5 keV at 4.55 s, where the EUV spectrum shows a discrete feature as plotted in the top panel of figure 2. After that, the plasma temperature rapidly began to drop near the center until the central temperature became almost zero at 4.85 s due to the formation of a hollow plasma as shown in the bottom panel of figure 2 (b). In this phase, low temperature plasma was still maintained in the edge region where peak temperature is about 400 eV. This is similar to the phenomenon we have already reported for Gd and Nd injections [12]. Following this drastic decrease in electron temperature, the feature of the EUV spectrum also dynamically changes, as shown in figure 2 (a). The broad quasicontinuum UTA structure is pronounced in the second panel where the peak electron temperature is about 1 keV. Further decrease in electron temperature leads to the narrowing of the UTA bandwidth and the shift of the UTA peak position to shorter wavelengths. Note that the intensity of the UTA feature is usually much higher than that of the discrete feature as shown in the vertical scale of figure 2 (a). Finally, the UTA bandwidth was narrowed to about 0.1 nm, as shown in the bottom panel. As a result, a characteristic double peak is apparently seen around 6.9 nm.

We have also measured temperature dependent Dy spectra in a similar way.

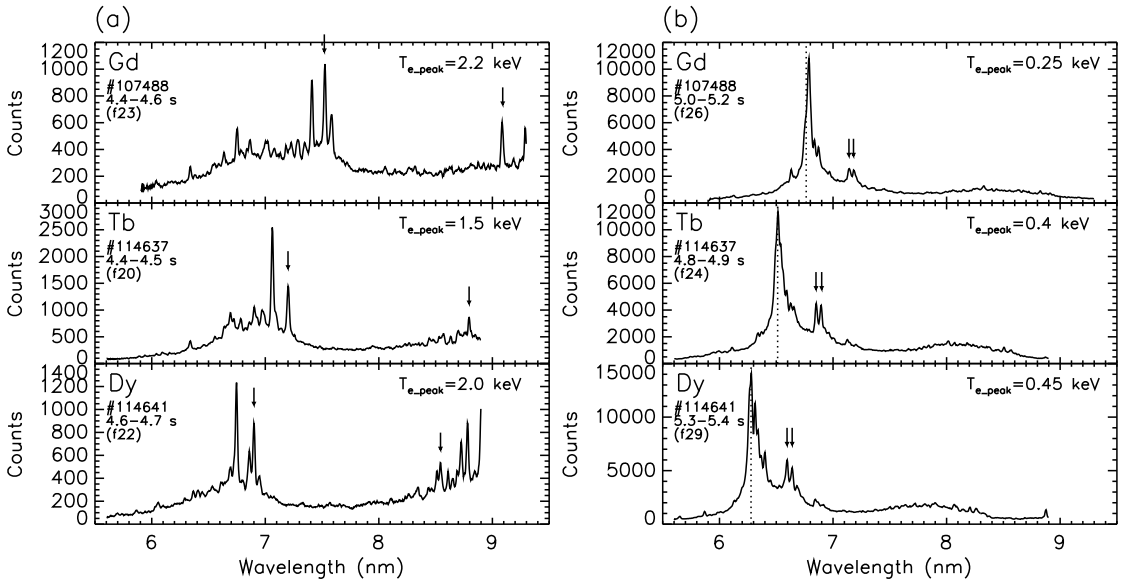

Figure 3. EUV spectra of lanthanide ions from Gd to Dy in (a) high temperature and (b) hollow temperature plasmas measured in the LHD. The representative peak electron temperatures corresponding to each spectrum are also shown in each panel. All of the arrows in (a) denote the identified emission lines from Cu-like ions, while those in (b) denote the lines of Ag-like ions. The vertical dotted lines in (b) represent the previously reported positions of the lines due to $4d^{10}\ {}^1S_0$ – $4d^9 4f\ {}^1P_1$ transition of Pd-like ions.

Together with the previously reported results for Gd, the EUV spectra in the (a) highest temperature and (b) hollow temperature plasmas are summarized for Gd, Tb and Dy in figure 3. The representative peak electron temperatures corresponding to each spectrum are also shown in each panel. The Z dependence of the positions of the prominent spectral lines and the UTA is clearly found in figure 3. The identified discrete lines of Cu-like ions are marked by arrows in figure 3 (a), and those of Ag-like ions in figure 3 (b). In addition, the previously reported positions of the lines due to $4d^{10}\ {}^1S_0$ – $4d^9 4f\ {}^1P_1$ transition of Pd-like ions are denoted by vertical dotted lines in figure 3 (b). These are discussed in detail in the next section.

4. Line identification

As reported in the previous article, we have already identified some of the discrete spectral lines of Gd ions shown in figure 3. In this study, we have tried to identify the observed discrete lines in the spectra of Tb and Dy ions based on comparisons with earlier studies and theoretical calculation by Hullac code [30]. Consequently, isolated lines of Ni- and Pd-like Tb and Dy ions could not be clearly identified because of low intensity or blending with the UTA feature. Indeed, the previously reported positions of

Table 1. Wavelengths of the identified lines of Cu-like Gd, Tb and Dy ions in the spectra shown in figure 3 (*a*). Experimental wavelengths in the present study (LHD) are listed with those in the previous publications and calculated with Hullac code. References: *a*–[21], *b*–[31], *c*–[32], *d*–[23].

		Wavelength (nm)		
Transition	Ion	LHD	previous	calculated
$3d^{10}4p\ ^2P_{1/2}$ – $3d^{10}4d\ ^2D_{3/2}$	Gd^{35+}	7.524	7.527[a], 7.5259[b], 7.5316[c]	7.524
	Tb^{36+}	7.202	—	7.208
	Dy^{37+}	6.901	6.905[d], 6.9080[c]	6.901
$3d^{10}4d\ ^2D_{3/2}$ – $3d^{10}4f\ ^2F_{5/2}$	Gd^{35+}	9.091	9.086[a], 9.0875[b], 9.0933[c]	9.109
	Tb^{36+}	8.795	—	8.827
	Dy^{37+}	8.543	8.5452[c]	8.561

the lines of Pd-like ions are marked by vertical dotted lines in figure 3 (b), which seems to be more intense in figure 3 than actual due to blending with lines of adjacent ion stages, and are difficult to discriminate. However, Cu-like ions and Ag-like ions which have relatively simple electronic configurations ($3d^{10}4s$ and $4d^{10}4f$) are well isolated and easily identified, as denoted by arrows in figure 3.

The observed wavelength range in this work was primarily tuned to the UTA of 4p-4d and 4d-4f transition arrays. Therefore, the 4s–4p resonance lines of Cu-like ions, which should be much more intense, are out of the wavelength range. For example, the wavelengths of the 4s $^2S_{1/2}$ – 4p $^2P_{3/2}$ transitions of Cu-like Gd^{35+} and Dy^{37+} have been experimentally reported to be 10.247 nm and 9.261 nm, respectively [21, 23], which are out of the wavelength range in this study. Therefore, the wavelength range in the present observation includes only 4p–4d and 4d–4f transitions between excited states of Cu-like ions. Table 1 lists the observed wavelengths of the lines due to $3d^{10}4p\ ^2P_{1/2}$ – $3d^{10}4d\ ^2D_{3/2}$ and $3d^{10}4d\ ^2D_{3/2}$ – $3d^{10}4f\ ^2F_{5/2}$ transitions for Gd–Dy, together with the experimental values in the previous articles [21, 23, 31, 32] except for Tb and those calculated with Hullac code. As shown, the wavelengths of these transitions for Gd and Dy are in very good agreement with the previous experimental values and the calculated ones. Though there are no experimental data available for Tb, the present values reasonably agree with those calculated in this study. Consequently, this study gives the initial experimental identifications of spectral lines of Cu-like Tb ions.

On the other hand, the observed wavelengths of 4d–4f doublet of Ag-like ions are summarized in table 2 together with those in the previous article [34] and those calculated with Hullac code. Though the present values agree well with the previous values, the calculated wavelengths systematically deviate 0.2–0.3 nm to shorter wavelengths from the measurements. This discrepancy could result from the theoretical method to calculate atomic structures of multi-electron systems. The parametric potential method adopted in the Hullac code does not necessarily give energy levels with sufficient accuracy for n=4–4 transitions, especially for inner-shell excited levels

Table 2. Wavelengths of the identified lines of Ag-like Gd, Tb and Dy ions in the spectra shown in figure 3 (*b*). Experimental wavelengths in the present study (LHD) are listed with those in the previous publications and calculated with Hullac code. Reference: *e*–[34].

		Wavelength (nm)		
Transition	Ion	LHD	previous	calculated
$4d^{10}4f\ ^2F_{7/2}$ – $4d^94f^2\ ^2G_{9/2}$	Gd^{17+}	7.140	7.1430[e]	6.838
	Tb^{18+}	6.852	6.8578[e]	6.587
	Dy^{19+}	6.595	6.5967[e]	6.349
$4d^{10}4f\ ^2F_{5/2}$ – $4d^94f^2\ ^2G_{7/2}$	Gd^{17+}	7.182	7.1853[e]	6.886
	Tb^{18+}	6.895	6.9029[e]	6.635
	Dy^{19+}	6.641	6.6437[e]	6.398

such as $4d^94f^2$ in this case. Although the inner-shell excitation could require a change in the parametric potential, the actual calculations cannot sufficiently reflect the condition. Therefore, the calculated wavelengths of $4d^{10}4f$–$4d^94f^2$ transition lines of Ag-like ions do not tend to agree with the measurements. We are planning to investigate further these atomic structures using another theoretical codes such as GRASP [35, 36]. The lines of the other 4d-4f transitions (^2F – ^2F, ^2F – ^2D) of Ag-like ions are expected to appear near the peak of the UTA together close to the line of Pd-like ions. These lines are blended and difficult to separate in the present study due to the lack of spectral resolution. We should compare the measured UTA feature with the collisional-radiative modeling in the near future. Nevertheless, the proximity of the sharp UTA peaks in figure 3 (b) to the expected positions of the lines of Ag-like and Pd-like ions indicates that the dominant emitters in the hollow plasmas are Ag-like, Pd-like and their neighboring ion stages.

5. Summary

We have systematically measured EUV spectra in the 6–9 nm region emitted by highly charged Gd, Tb and Dy ions in optically thin plasmas produced in the LHD. The observed spectral feature has drastically changed following the rapid drop in electron temperature after the heating power was reduced. The discrete spectral feature including the lines of Cu-like ions is observed under the peak temperatures above 1.5 keV before the temperature drop. As the peak temperature drops, the spectral feature rapidly changes into UTA feature and its positions shift to shorter wavelengths, and then finally results in an extremely narrowed UTA feature with Ag-like doublet lines under the peak temperatures less than 450 eV. Some of the lines of Cu-like and Ag-like ions have been identified as n=4–4 transitions by comparisons with the previous experimental works and theoretical calculations. In particular, two lines of 4p–4d and 4d–4f transitions of Cu-like Tb^{36+} have been experimentally identified for the first time in this study. The identifications suggest that the injected lanthanide elements would be ionized up to Cu-

like stages in the highest temperature case, while Ag- and Pd-like ions are dominant emitters in the lowest temperature case when the hollow plasmas are formed. Atomic structure calculations and construction of collisional-radiative modeling using Hullac code are now underway including wider range of charge states to give an insight into the observed temporal evolutions of the appearance of the UTA, which will be reported in a separate paper.

Acknowledgments

The authors acknowledge the LHD experiment group for their assistance. This work was carried out with the support and under the auspices of the NIFS collaboration research program (NIFS12KLPF025). This work was supported also by a Grant-in-Aid for Young Scientists (B) from Japan Society for the Promotion of Science.

References

[1] Churilov S S, Kildiyarova R R, Ryabtsev A N and Sadovsky S V 2009 *Phys. Scr.* **80** 045303
[2] Kilbane D and O'Sullivan G 2010 *J. Appl. Phys.* **108** 104905
[3] Otsuka T, Kilbane D, White J, Higashiguchi T, Yugami N, Yatagai T, Jiang W, Endo A, Dunne P and O'Sullivan G 2010 *Appl. Phys. Lett.* **97** 111503
[4] Li B, Otsuka T, Higashiguchi T, Yugami N, Jiang W, Endo A, Dunne P and O'Sullivan G 2012 *Appl. Phys. Lett.* **101** 013112
[5] O'Sullivan G and Carroll P K 1981 *J. Opt. Soc. Am.* **71** 227
[6] Koike F and Fritzsche S 2007 *Rad. Phys. Chem.* **76** 404
[7] Kato T *et al* 2008 *J. Phys. B: At. Mol. Opt. Phys.* **41** 035703
[8] Suzuki C *et al* 2009 *J. Phys. Conf. Ser.* **163** 012019
[9] Suzuki C *et al* 2010 *J. Phys. B: At. Mol. Opt. Phys.* **43** 074027
[10] Harte C S *et al* 2010 *J. Phys. B: At. Mol. Opt. Phys.* **43** 205004
[11] Suzuki C *et al* 2011 *J. Phys. B: At. Mol. Opt. Phys.* **44** 175004
[12] Suzuki C, Koike F, Murakami I, Tamura N and Sudo S 2012 *J. Phys. B: At. Mol. Opt. Phys.* **45** 135002
[13] Suzuki C *et al* 2014 *Phys. Scr.* **89** 114009
[14] Carroll P K and O'Sullivan G 1982 *Phys. Rev.* A **25** 275
[15] Zeng G M, Daido H, Nishikawa T, Takabe H, Nakayama S, Aritome H, Murai K, Kato Y, Nakatsuka M and Nakai S 1994 *J. Appl. Phys.* **75** 1923
[16] Mandelbaum P, Finkenthal M, Schwob J L and Klapisch M 1987 *Phys. Rev.* A **35** 5051
[17] Finkenthal M *et al* 1986 *J. Appl. Phys.* **59** 3644
[18] Finkenthal M, Moos H W, Bar-Shalom A, Spector N, Zigler A and Yarkoni E 1988 *Phys. Rev.* A **38** 288
[19] Finkenthal M, Lippmann S, Huang L K, Moos H W, Lee Y T, Spector N, Zigler A and Yarkoni E 1990 *Phys. Scr.* **41** 445
[20] Fournier K B, Goldstein W H, Osterheld A, Finkenthal M, Lippmann S, Huang L K, Moos H W and Spector N 1994 *Phys. Rev.* A **50** 2248
[21] Kilbane D, O'Sullivan G, Gillaspy J D, Ralchenko Yu and Reader J 2012 *Phys. Rev.* A **86** 042503
[22] Ohashi H, Sakaue H A and Nakamura N 2013 *Phys. Scr.* **T156** 014013
[23] Kilbane D, O'Sullivan G, Podpaly Y A, Gillaspy J D, Reader J and Ralchenko Yu 2014 *Eur. Phys. J. D* **68** 222
[24] Komori A *et al* 2009 *Nucl. Fusion* **49** 104015

[25] Sudo S *et al* 2002 *Plasma Phys. Control. Fusion* **44** 129
[26] Sudo S and Tamura N 2012 *Rev. Sci. Instrum.* **83** 023503
[27] Narihara K, Yamada I, Hayashi H and Yamauchi K 2001 *Rev. Sci. Instrum.* **72** 1122
[28] Yamada K *et al* 2010 *Rev. Sci. Instrum.* **81** 10D522
[29] Schwob J L, Wouters A W, Suckewer S and Finkenthal M 1987 *Rev. Sci. Instrum.* **58** 1601
[30] Bar-Shalom A, Klapisch K and Oreg J 2011 *J. Quant. Spectrosc. Radiat. Transfer* **71** 169
[31] Doschek G A, Feldman U, Brown C M, Seely J F, Ekberg J O, Behring W E and Richardson M C 1988 *J. Opt. Soc. Am.* B **5** 243
[32] Reader J and Luther G 1981 *Phys. Scr.* **24** 732
[33] Bar-Shalom A, Klapisch K and Oreg J 2011 *J. Quant. Spectrosc. Radiat. Transfer* **71** 169
[34] Sugar J and Kaufman V 1981 *Phys. Scr.* **24** 742
[35] Parpia F A, Fischer C F and Grant I P 1996 *Comput. Phys. Commun.* **94** 249
[36] Fritzsche S 2012 *Comput. Phys. Commun.* **183** 1525